SAND2018-5675C

Computational Peridynamics

David Littlewood
Sandia National Laboratories

John Foster
University of Texas

Pablo Seleson
Oak Ridge National Laboratory

18th U.S. National Congress for Theoretical and Applied Mechanics

June 4-9, 2018

Short Course
Peridynamic Theory of Solid Mechanics

Computational Peridynamics

Outline

- Ingredients of a peridynamics simulation
  - Governing equations
  - Constitutive model, bond failure law
  - Contact model
  - Discretization
  - Time integrator
- Surface effect in peridynamic simulations
- Estimation of the maximum stable time step for dynamic simulations
- Convergence of peridynamic models
- Demonstration of meshfree peridynamics for model analysis
- Modeling damage and failure

Ingredients for computational peridynamics

- Governing equations
   - Continuum form of the balance of linear momentum

$$\rho(\mathbf{x})\ddot{\mathbf{u}}(\mathbf{x}, t) = \int_{\mathscr{B}} \left\{ \underline{\mathbf{T}}[\mathbf{x}, t] \langle \mathbf{x}' - \mathbf{x} \rangle - \underline{\mathbf{T}}'[\mathbf{x}', t] \langle \mathbf{x} - \mathbf{x}' \rangle \right\} \, dV_{\mathbf{x}'} + \mathbf{b}(\mathbf{x}, t)$$

    - Semi-discrete form: meshless discretization of the strong form

$$\rho(\mathbf{x})\ddot{\mathbf{u}}_h(\mathbf{x}, t) = \sum_{i=0}^{N} \left\{ \underline{\mathbf{T}}[\mathbf{x}, t] \langle \mathbf{x}'_i - \mathbf{x} \rangle - \underline{\mathbf{T}}'[\mathbf{x}'_i, t] \langle \mathbf{x} - \mathbf{x}'_i \rangle \right\} \Delta V_{\mathbf{x}'_i} + \mathbf{b}(\mathbf{x}, t)$$

- Boundary and initial conditions
- Constitutive model
- Bond failure law
- Contact model

- Discretization
- Time integration
    - Explicit
    - Implicit
- Pre- and post-processing

Meshfree peridynamic model of an expanding, fragmenting cylinder

Damage
1
0.75
0.5
0.25
0
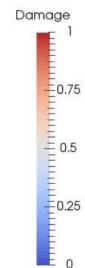
S.A. Silling. Reformulation of elasticity theory for discontinuities and long-range forces. *Journal of the Mechanics and Physics of Solids*, 48:175-209, 2000.

S.A. Silling and E. Askari. A meshfree method based on the peridynamic model of solid mechanics. *Computers and Structures*, 83:1526-1535, 2005.
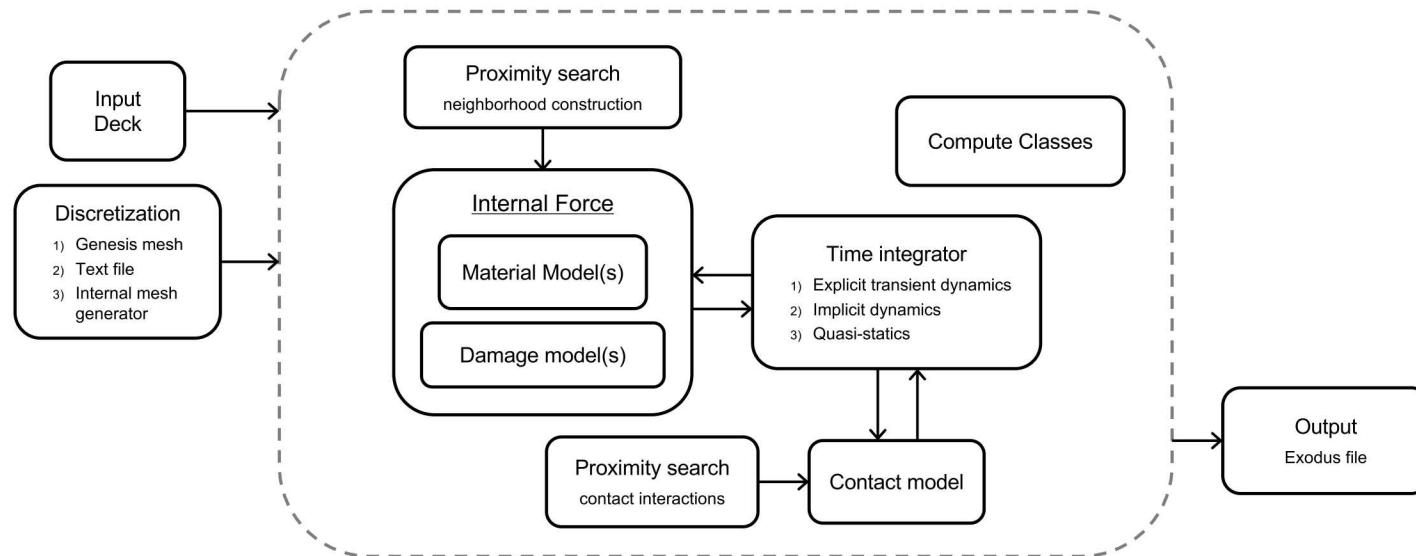
Short Course
Peridynamic Theory of Solid Mechanics

Model for a peridynamics simulation code

Constitutive models

- Bond-based models
  - Direct pairwise interactions
- State-based models
  - Multi-point interactions
- Correspondence models
  - Wrapper for classic stress-strain models

Example: Linear peridynamic solid [Silling]

- State-based model
- Deformation decomposed into deviatoric and dilatational components

$$\theta = \frac{3}{m} \int_{\mathcal{H}} (\underline{\omega}\, \underline{x}) \cdot \underline{e} \, dV \qquad \underline{e}^d = \underline{e} - \frac{\theta\, \underline{x}}{3}$$

- Magnitude of pairwise force density given by

$$\underline{t} = \frac{3k\theta}{m} \underline{\omega}\, \underline{x} + \frac{15\mu}{m} \underline{\omega}\, \underline{e}^{\mathrm{d}}$$

S.A. Silling, M. Epton, O. Weckner, J. Xu, and E. Askari, Peridynamic states and constitutive modeling, *Journal of Elasticity*, 88, 2007.

Software implementation of the Linear Peridynamic Solid

Algorithm 1 The initialization routine for a *linear peridynamic solid* material with a Gaussian influence function.

1: **procedure** LINEAR PERIDYNAMIC SOLID INITIALIZATION
2:    ▷ Compute the weighted volume for each node.
3:    **for each** node i **do**
4:       $m_i \leftarrow 0$
5:       **for each** node j in neighbor list for node i **do**
6:          $\boldsymbol{\xi} \leftarrow \mathbf{x}_j - \mathbf{x}_i$
7:          $\underline{\omega} \leftarrow \exp\left(-\frac{|\boldsymbol{\xi}|^2}{\delta^2}\right)$
8:          $m_i \leftarrow m_i + \underline{\omega}\,|\boldsymbol{\xi}|^2\,\Delta V_j$
9:       **end for**
10:    **end for**
11: **end procedure**

Algorithm 2 Routine for calculation of the internal force density for a *linear peridynamic solid* material with a Gaussian influence function.

1: **procedure** LINEAR PERIDYNAMIC SOLID INTERNAL FORCE
2:    ▷ Initialize the global force density vector to zero.
3:    **for each** node i **do**
4:       $\mathbf{f}_i \leftarrow 0$
5:    **end for**
6:    ▷ Compute the dilatation for each node.
7:    **for each** node i **do**
8:       $\theta_i \leftarrow 0$
9:       **for each** node j in neighbor list for node i **do**
10:          $\boldsymbol{\xi} \leftarrow \mathbf{x}_j - \mathbf{x}_i$
11:          $\boldsymbol{\eta} \leftarrow \mathbf{u}_j - \mathbf{u}_i$
12:          $\underline{\omega} \leftarrow \exp\left(-\frac{|\boldsymbol{\xi}|^2}{\delta^2}\right)$
13:          $\underline{e} \leftarrow |\boldsymbol{\xi} + \boldsymbol{\eta}| - |\boldsymbol{\xi}|$
14:          $\theta_i \leftarrow \theta_i + \frac{3}{m_i}\,\underline{\omega}\,|\boldsymbol{\xi}|\,\underline{e}\,\Delta V_j$
15:       **end for**
16:    **end for**
17:    ▷ Compute the pairwise contributions to the global force density vector.
18:    **for each** node i **do**
19:       **for each** node j in neighbor list for node i **do**
20:          $\boldsymbol{\xi} \leftarrow \mathbf{x}_j - \mathbf{x}_i$
21:          $\boldsymbol{\eta} \leftarrow \mathbf{u}_j - \mathbf{u}_i$
22:          $\underline{\omega} \leftarrow \exp\left(-\frac{|\boldsymbol{\xi}|^2}{\delta^2}\right)$
23:          $\underline{e} \leftarrow |\boldsymbol{\xi} + \boldsymbol{\eta}| - |\boldsymbol{\xi}|$
24:          $\underline{e}^d \leftarrow \underline{e} - \frac{\theta_i |\boldsymbol{\xi}|}{3}$
25:          $\underline{t} \leftarrow \frac{3}{m_i}\,k\,\theta_i\,\underline{\omega}\,|\boldsymbol{\xi}| + \frac{15\mu}{m_i}\underline{\omega}\,\underline{e}^d$
26:          $\underline{\mathbf{M}} \leftarrow \frac{\boldsymbol{\xi}+\boldsymbol{\eta}}{|\boldsymbol{\xi}+\boldsymbol{\eta}|}$
27:          $\mathbf{f}_i \leftarrow \mathbf{f}_i + \underline{t}\,\underline{\mathbf{M}}\,\Delta V_j$
28:          $\mathbf{f}_j \leftarrow \mathbf{f}_j - \underline{t}\,\underline{\mathbf{M}}\,\Delta V_i$
29:       **end for**
30:    **end for**
31: **end procedure**

David J. Littlewood. Roadmap for Peridynamic Software Implementation. SAND Report 2015-9013. Sandia National Laboratories, Albuquerque, NM and Livermore, CA, 2015.

Bond failure law

- Critical stretch [Silling]
    - Brittle failure
    - Critical stretch value determined from the material's energy release rate
- Energy-based approach [Foster]
- Ductile failure models [Silling]

Example: Critical stretch law

- Bond fails irreversibly when critical stretch is exceeded

$$s_{\max} = \frac{y_{\max} - x}{x}$$

$$d = \begin{cases} 0 & \text{if} & s_{\max} < s_o \\ 1 & \text{if} & s_{\max} \geq s_0 \end{cases}$$

S.A. Silling, M. Epton, O. Weckner, J. Xu, and E. Askari, Peridynamic states and constitutive modeling, *Journal of Elasticity*, 88, 2007.

Software implementation of the
Critical Stretch Bond Failure Law

Algorithm 3 Routine for evaluation of the *critical stretch* bond failure law. Bond damage values, d_{ij}, are initialized to zero at the beginning of the simulation and set to a value of one if the bond stretch exceeds the specified critical value.

```
 1: procedure CRITICAL STRETCH BOND FAILURE
 2:     for each node i do
 3:         ▷ Evaluate the stretch of each bond.
 4:         for each node j in neighbor list for node i do
 5:             ξ ← x_j − x_i
 6:             η ← u_j − u_i
 7:             s = (|ξ+η|−|ξ|) / |ξ|
 8:             ▷ Check the bond stretch against the critical value.
 9:             if s ≥ s_o then
10:                 d_ij = 1.0
11:             end if
12:         end for
13:     end for
14: end procedure
```

$\boldsymbol{\xi} \leftarrow \mathbf{x}_j - \mathbf{x}_i$

$\boldsymbol{\eta} \leftarrow \mathbf{u}_j - \mathbf{u}_i$

$s = \dfrac{|\boldsymbol{\xi}+\boldsymbol{\eta}|-|\boldsymbol{\xi}|}{|\boldsymbol{\xi}|}$

if $s \geq s_o$ then

$d_{ij} = 1.0$

Modeling contact

- Contact algorithms involve two distinct steps:
  - Proximity search
  - Enforcement

- The majority of meshfree peridynamic simulations to date have utilized the short-range force approach of Silling

- Local contact models have also been applied to peridynamic simulations
  - Iterative penalty approach to disallow interpenetration and minimize contact gap

- Contact modeling remains an open research topic in peridynamics
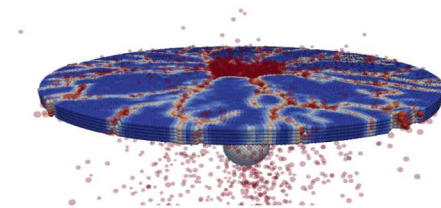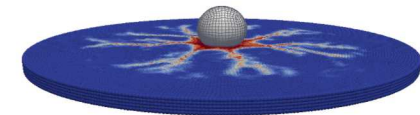
Simulation of brittle fracture

1. Silling, S.A. and Askari, E. A meshfree method based on the peridynamic model of solid mechanics. *Computers and Structures* 83:1526-1535, 2005.
2. SIERRA Solid Mechanics Team, Sierra/SolidMechanics 4.22 user's guide, SAND Report 2011-7597, Sandia National Laboratories, Albuquerque, NM and Livermore, CA, 2011.

Short Course
Peridynamic Theory of Solid Mechanics

Short-range force contact models

- Spring-like repulsive force
- Active when relative distance is smaller than the prescribed contact radius
- Does not require explicit definition of contact surfaces
- Interpenetration is possible (high velocity, node misalignment)
- Friction may be incorporated by decomposing relative motion into normal and tangential components

Example of a short-range force contact model

Force is zero if distance between nodes is greater than d_{ij}

$$d_{ij} = \min\left\{\beta|\mathbf{x}_j - \mathbf{x}_i|, \alpha(r_i + r_j)\right\}$$

Short-range force includes static and dynamic components

$$\mathbf{f}_{\text{static}} = A\, C_{ij} \left(\frac{d - |\mathbf{y}_j - \mathbf{y}_i|}{d}\right) \Delta V_i\, \Delta V_j\, \mathbf{M}_{ij}$$

$$C_{ij} = \frac{18k}{\pi\delta^4} \qquad \mathbf{M}_{ij} = \frac{\mathbf{y}_j - \mathbf{y}_i}{|\mathbf{y}_j - \mathbf{y}_i|}$$

$$\mathbf{f}_{\text{damping}} = \epsilon\, \gamma_c\, v_{ij}\, \mathbf{M}_{ij}$$

$$v_{ij} = (\mathbf{v}_j - \mathbf{v}_i) \cdot \mathbf{M}_{ij}$$

$$\gamma_c = 2\sqrt{A\, C_{ij}\, \Delta V_i\, \Delta V_j\, \bar{m}}$$

Illustration of short range force and standard bond force
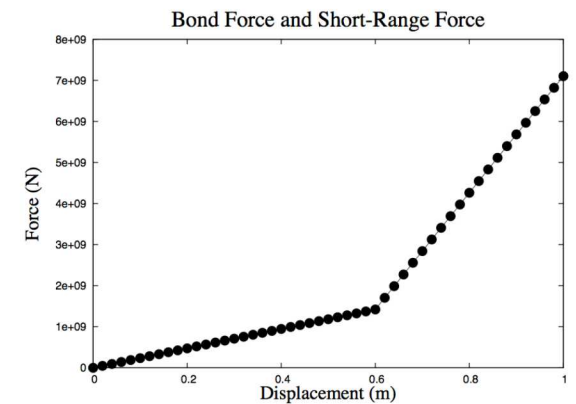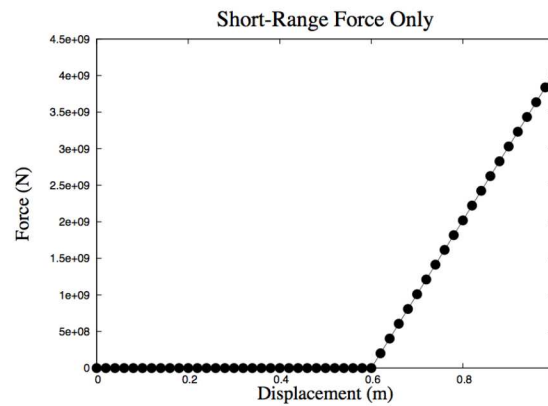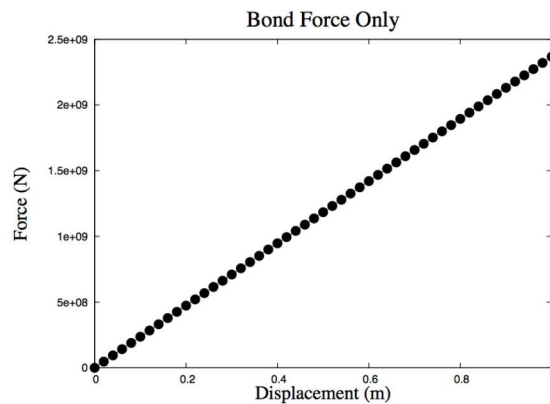
Applying a traditional (local) contact model to peridynamics

- Contact algorithm operates on planar facets

- Peridynamics algorithm operates on sphere elements

- Lofted geometry allows for coupling of peridynamics and contact algorithm

Initial hex mesh   Conversion to sphere mesh   Create planar facets for contact algorithm
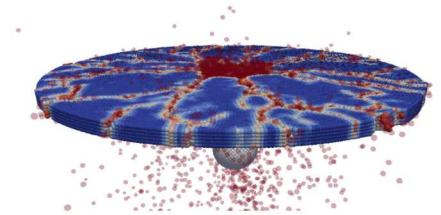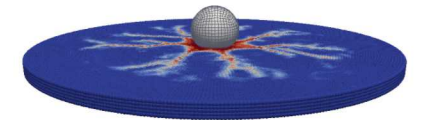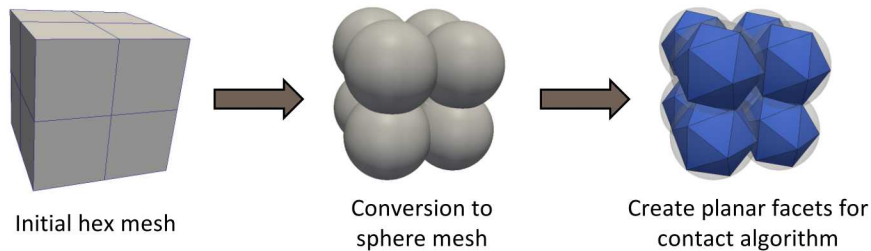
Simulation of brittle fracture

D. J. Littlewood. Simulation of dynamic fracture using peridynamics, finite element modeling, and contact. In *Proceedings of the ASME 2010 International Mechanical Engineering Congress and Exposition (IMECE)*, Vancouver, British Columbia, Canada, 2010.

SIERRA Solid Mechanics Team. Sierra/SolidMechanics 4.36 user's guide. SAND Report 2015-2199, Sandia National Laboratories, Albuquerque, NM and Livermore, CA.

Computational Peridynamics
1. Ingredients of a peridynamic simulation

Challenges with contact and nonlocal models

Simple test: To bars in contact and under compression
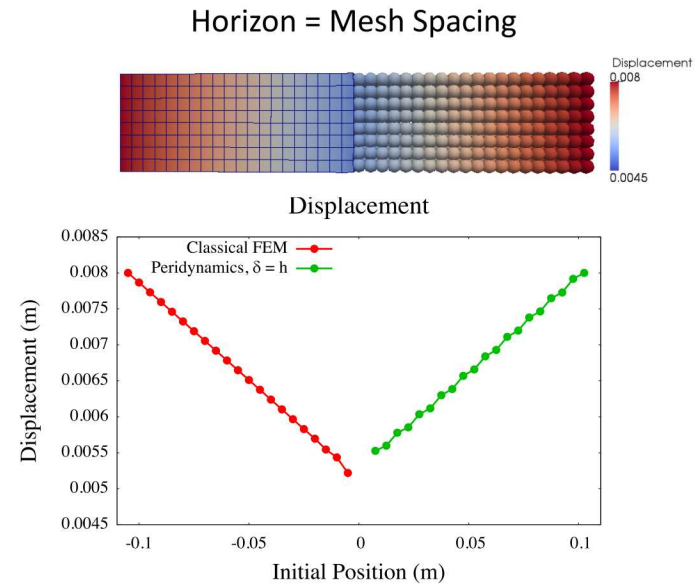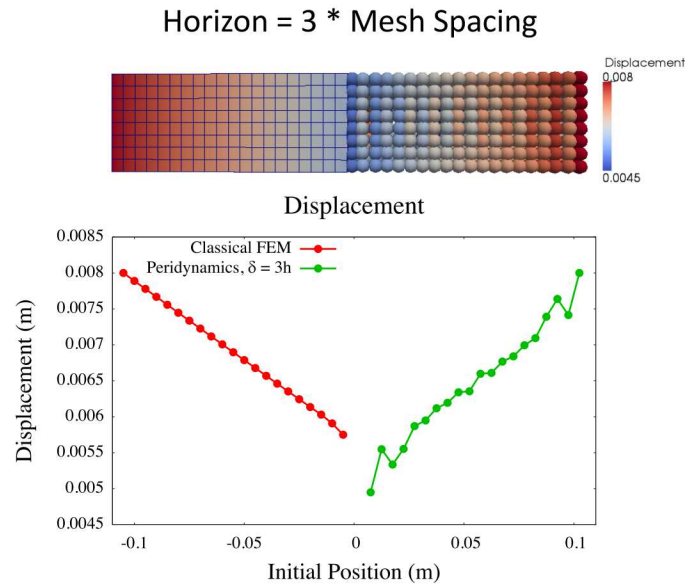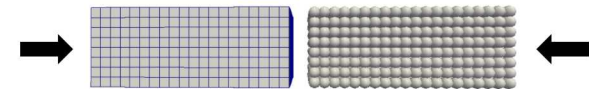
Horizon = 3 * Mesh Spacing

Horizon = Mesh Spacing

Meshfree discretizations for peridynamics

- Meshfree discretization is defined by nodal volumes: **(x, y, z, V)**

- Each nodal volumes is assigned a material model, etc.
  - Nodal volumes may be grouped into "blocks" to simplify bookkeeping

- Example approaches for generating a meshfree discretization:
  - Simulation code internal mesh generator
  - Pre-processing script to generate (x,y,z,V) data
  - Conversion of a FEM hex/tet mesh to nodal volumes

- Concerns specific to peridynamics:
  - A variable horizon is generally not supported in peridynamics
  - Discretization can be nonuniform, but large variations in V can produce undesirable results
  - Boundary conditions are generally applied over a volumetric region; bookkeeping can be challenging, thin layers can cause difficulty
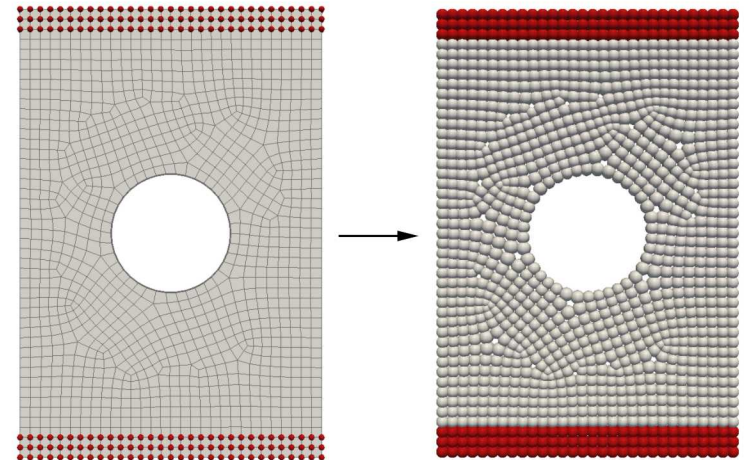
Conversion of a FEM mesh to a meshfree discretization

- Node sets defined in the original hex/tet mesh must be transferred to meshless discretization
  - Elements are preserved (one-to-one map) but nodes in the FEM mesh are not preserved
- A mechanism is required for treating small features, controlling visibility between material points
  - A so-called bond filter may be used to disallow pairwise interactions
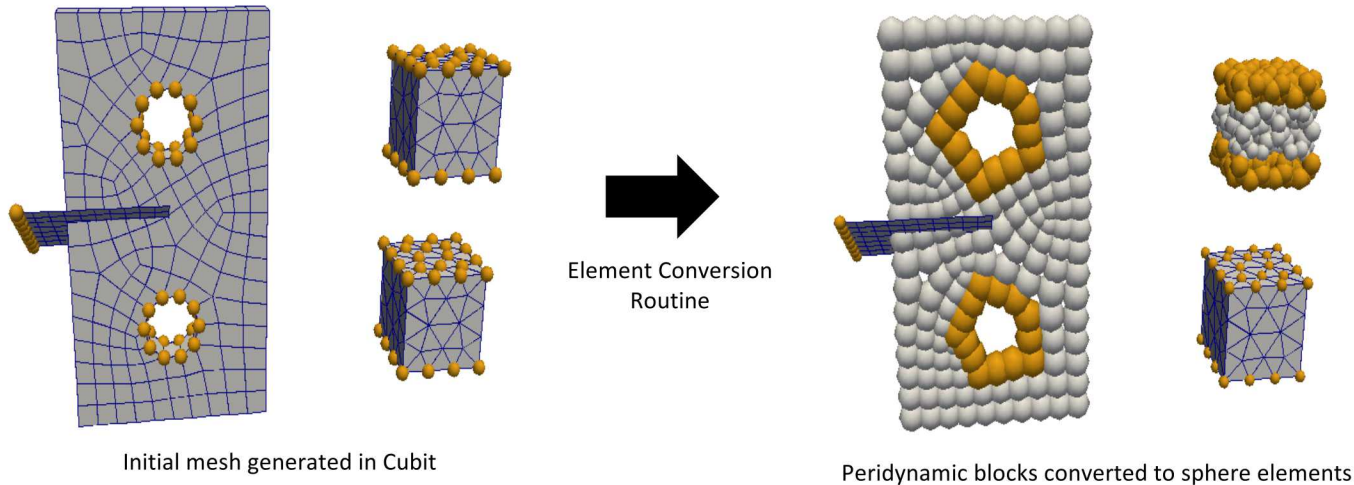
Element Conversion Routine

Initial mesh generated in Cubit

Peridynamic blocks converted to sphere elements

Short Course
Peridynamic Theory of Solid Mechanics

Time integration for computational solid mechanics

- Explicit integration (dynamics): Velocity-Verlet, a.k.a. leapfrog

  - Well suited for modeling pervasive damage

  - Does not require the solution of a global system of equations

  - Conditionally stable, requires small time step

  - Equivalent to Newmark Beta with Beta = 0, gamma = 0.5

- Implicit integration for quasi-statics

  - Assumes that acceleration is zero everywhere, solve for equilibrium

  - Wave propagation is neglected

  - Requires solution of a global system of equations

  - Care must be taken w.r.t. rigid body modes

- Implicit integration for dynamics

  - Newmark Beta

  - Requires solution of a global system of equations

Explicit time integration

- Appropriate for dynamic problems and those with pervasive material failure

$$\rho(\mathbf{x})\ddot{\mathbf{u}}_h(\mathbf{x}, t) = \sum_{i=0}^{N} \left\{ \underline{\mathbf{T}}[\mathbf{x}, t] \langle \mathbf{x}_i' - \mathbf{x} \rangle - \underline{\mathbf{T}}'[\mathbf{x}_i', t] \langle \mathbf{x} - \mathbf{x}_i' \rangle \right\} \Delta V_{\mathbf{x}_i'} + \mathbf{b}(\mathbf{x}, t)$$

- Conditionally stable

- Requires estimate of the critical time step

- Requires many small time steps

- Easy to implement

- Does not require solution of global system of equations

Algorithm 1 Velocity Verlet

1: $\mathbf{v}^{n+1/2} = \mathbf{v}^n + \frac{\Delta t}{2}\mathbf{M}^{-1}(\mathbf{f}^n + \mathbf{b}^n)$
2: $\mathbf{u}^{n+1} = \mathbf{u}^n + \Delta t \mathbf{v}^{n+1/2}$
3: $\mathbf{v}^{n+1} = \mathbf{v}^{n+1/2} + \frac{\Delta t}{2}\mathbf{M}^{-1}(\mathbf{f}^{n+1} + \mathbf{b}^{n+1})$

Implicit time integration

- Unconditionally stable

- Allows for large time steps

- Suitable for solution of static and quasi-static problems

- Suitable for implicit dynamics

- Requires solution of system of equations involving current and future configurations

  - Generally nonlinear

  - Newton-like methods require tangent stiffness matrix

  - Matrix-free schemes offer a promising alternative approach (e.g., Jacobian-Free Newton-Krylov)

S. A. Silling. Linearized theory of peridynamic states. *Journal of Elasticity*, 99:85–111, 2010.

J. A. Mitchell. A nonlocal, ordinary, state-based plasticity model for peridynamics. SAND Report 2011-3166, Sandia National Laboratories, Albuquerque, NM and Liver- more, CA, 2011.

M.L. Parks, D.J. Littlewood, J.A. Mitchell, and S.A. Silling, Peridigm Users' Guide v1.0.0. Sandia Report SAND2012-7800, 2012.

Brothers, M.D., Foster, J.T., and Millwater, H.R. A comparison of different methods for calculating tangent-stiffness matrices in a massively parallel computational peridynamics code. *Computer Methods in Applied Mechanics and Engineering* 279:247-267, 2014.

David J. Littlewood. Roadmap for Peridynamic Software Implementation. SAND Report 2015-9013. Sandia National Laboratories, Albuquerque, NM and Livermore, CA, 2015.

Short Course
Peridynamic Theory of Solid Mechanics

Computational Peridynamics

1. Ingredients of a peridynamic simulation

The tangent stiffness matrix

- Approaches for construction:
  - Analytic (i.e., peridynamic modulus state)
  - Finite difference
  - Automatic differentiation

- Tangent is expensive
  - Expensive to construct
  - Expensive to store
  - Expensive to apply

- Number of nonzeros is directly related to the number of peridynamic bonds
  - Nonzero entry for all bonded nodes
  - Nonzero entry for all nodes that are bonded to a common node (state based)

Algorithm 1 Construction of the tangent stiffness matrix by central finite difference.

1: **procedure** TANGENT STIFFNESS MATRIX
2:   ▷ Initialize the tangent stiffness matrix to zero.
3:   $\mathbf{K} \leftarrow \mathbf{0}$
4:   ▷ Traverse each node in the discretization.
5:   **for each** node i **do**
6:     $\{traversal\ list\} \leftarrow$ node i and all neighbors of node i
7:     **for each** node j in $\{traversal\ list\}$ **do**
8:       ▷ Evaluate the force state at $\mathbf{x}_i$ under perturbations of displacement.
9:       **for each** displacement degree of freedom r at node j **do**
10:         $\underline{\mathbf{T}}^{\epsilon+} \leftarrow \underline{\mathbf{T}}[\mathbf{x}_i](\mathbf{u} + \boldsymbol{\epsilon}^r)$
11:         $\underline{\mathbf{T}}^{\epsilon-} \leftarrow \underline{\mathbf{T}}[\mathbf{x}_i](\mathbf{u} - \boldsymbol{\epsilon}^r)$
12:         ▷ Evaluate pairwise forces under perturbations of displacement.
13:         **for each** node k in neighbor list of node i **do**
14:           $\boldsymbol{f}^{\epsilon+} \leftarrow \underline{\mathbf{T}}^{\epsilon+}\langle\mathbf{x}_k - \mathbf{x}_i\rangle\ \Delta V_i\ \Delta V_k$
15:           $\boldsymbol{f}^{\epsilon-} \leftarrow \underline{\mathbf{T}}^{\epsilon-}\langle\mathbf{x}_k - \mathbf{x}_i\rangle\ \Delta V_i\ \Delta V_k$
16:           $\boldsymbol{f}^{\text{diff}} \leftarrow \boldsymbol{f}^{\epsilon+} - \boldsymbol{f}^{\epsilon-}$
17:           **for each** degree of freedom s at node k **do**
18:             $\mathrm{K}_{sr} \leftarrow \mathrm{K}_{sr} + \frac{f_s^{\text{diff}}}{2\epsilon}$
19:           **end for**
20:         **end for**
21:       **end for**
22:     **end for**
23:   **end for**
24: **end procedure**

Computational Peridynamics

Outline

- Ingredients of a peridynamics simulation
  - Governing equations
  - Constitutive model, bond failure law
  - Contact model
  - Discretization
  - Time integrator
- **Surface effect in peridynamic simulations**
- Estimation of the maximum stable time step for dynamic simulations
- Convergence of peridynamic models
- Demonstration of meshfree peridynamics for model analysis
- Modeling damage and failure

The peridynamic surface effect is a significant concern for engineering applications

- The majority of peridynamic material models were derived based on bulk response
- Material points close to the surface have a reduced nonlocal region (fewer bonds) relative to material points in the bulk
- Ordinary peridynamic material models exhibit inconsistencies at the surface

Axial Displacement

Stored Elastic Energy

Stress versus Strain
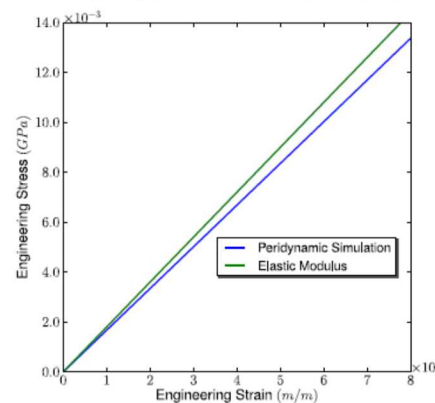
Root problem

An important subset of peridynamic models assumes that a full neighborhood of bonds is present

Surface

In the bulk

Missing bonds
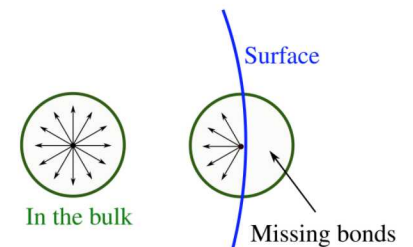
[Images courtesy John Mitchell]

Sandia National Laboratories

OAK RIDGE National Laboratory

**Short Course
Peridynamic Theory of Solid Mechanics**

One possible approach to mitigating the surface effect

- **Position-Aware Linear Solid** (PALS) constitutive model takes proximity to free surfaces into account

$$W = \frac{1}{2}K\theta^2 + \mu(\underline{\sigma\varepsilon}) \bullet \underline{\varepsilon}, \qquad \theta = (\underline{\omega}|X|) \bullet \underline{e}$$

- Coefficients σ and ω are determined for each point in the discretized model

- Calculation of σ and ω ensures that the expected strain energy is recovered for a set of *matching deformations*

J. Mitchell, S. Silling, and D. Littlewood. A position-aware linear solid (PALS) model for isotropic elastic materials. *Journal of Mechanics of Materials and Structures* 10(5):539-557, 2015.

Example calculation

PALS model accurately recovers elastic modulus in tensile test

Computational Peridynamics

Outline

- Ingredients of a peridynamics simulation
  - Governing equations
  - Constitutive model, bond failure law
  - Contact model
  - Discretization
  - Time integrator
- Surface effect in peridynamic simulations
- **Estimation of the maximum stable time step for dynamic simulations**
- Convergence of peridynamic models
- Demonstration of meshfree peridynamics for model analysis
- Modeling damage and failure

Candidate approaches for estimating the maximum stable time step

- Courant-Friedrichs-Lewy (CFL) condition

$$c = \sqrt{\frac{k}{\rho}} \qquad \Delta t \leq \frac{\Delta x}{c}$$

- Approach of Silling and Askari for microelastic materials (von Neumann analysis)

$$\Delta t_c = \sqrt{\frac{2\rho}{\sum_p V_p C_{ip}}} \qquad C_{ip} = |\mathbf{C}(x_p - x_i)| = \left|\frac{\partial \mathbf{f}}{\partial \boldsymbol{\eta}}\right|$$

- Global estimate using eigenvalue analysis (via Lanczos method)

$$\mathbf{M}\ddot{\mathbf{u}} + \mathbf{K}\mathbf{u} = \mathbf{f} \qquad (\mathbf{K} - \lambda\mathbf{M})\mathbf{x} = 0 \qquad \Delta t_c = \frac{2}{\sqrt{\lambda}}$$

Littlewood, D.J., Thomas, J.D., and Shelton, T.R. Estimation of the critical time step for peridynamic models. Presented at the SIAM Conference on Mathematical Aspects of Materials Science, Philadelphia, Pennsylvania, 2013.

Sandia National Laboratories   OAK RIDGE National Laboratory

Short Course
Peridynamic Theory of Solid Mechanics

- Critical time step for simulation of wave propagation
    - Compared approaches for estimating the maximum stable time step against empirical observations
    - CFL limit with element size as the length scale, and the method of Silling & Askari were conservative
    - Lanczos method was very accurate (but expensive)
    - CFL limit with the horizon as the length scale was unstable

Fixed displacement in longitudinal direction

Initial velocity in longitudinal direction

Velocity (cm/s)
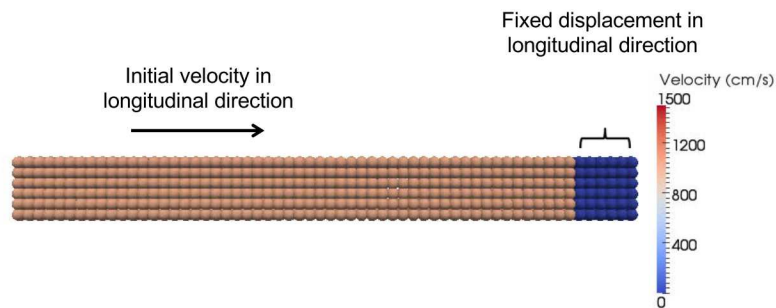
Time Step	Kinetic Energy
0.1 μs	3.51 J
0.2 μs	3.51 J
0.3 μs	3.51 J
0.4 μs	3.51 J
0.5 μs	14.1 J
0.6 μs	NaN
0.7 μs	NaN
0.8 μs	NaN
0.9 μs	NaN
1.0 μs	1.75e+299 J

Silling and Askari
max. time step = 0.241 µs
max. kinetic energy = 3.51 J

CFL Limit (element size)
max. time step = 0.329 µs
max. kinetic energy = 3.51 J

Empirical Observation
max. time step = 0.499 µs
max. kinetic energy = 3.51 J

Global Lanczos
max. time step = 0.500 µs
max. kinetic energy = 3.51 J

CFL Limit (horizon)
max. time step = 1.00 µs
max. kinetic energy = unstable

Time Step	Percentage of Broken Bonds	Maximum Kinetic Energy ($t > 10\ \mu s$)
0.01 μs	44.3 %	3.83 kJ
0.1 μs	44.5 %	3.82 kJ
0.2 μs	44.7 %	3.82 kJ
0.3 μs	45.3 %	3.82 kJ
0.4 μs	45.3 %	3.82 kJ
0.5 μs	45.4 %	3.82 kJ
0.6 μs	46.7 %	3.81 kJ
0.7 μs	49.1 %	3.83 kJ
0.8 μs	73.5 %	3.82 kJ
0.9 μs	95.3 %	4.39 kJ
1.0 μs	99.1 %	6.40 kJ

Silling and Askari

max. time step = 0.290 µs
percentage of broken bonds = 44.7 %
max. kinetic energy = 3.82 kJ

CFL Limit (element size)

max. time step = 0.395 µs
percentage of broken bonds = 45.3 %
max. kinetic energy = 3.51 J

Global Lanczos

max. time step = 0.682 µs
percentage of broken bonds = 46.0 %
max. kinetic energy = 3.83 kJ

Empirical Observation

max. time step = 0.707 µs
percentage of broken bonds = 50.0 %
max. kinetic energy = 3.83 kJ

CFL Limit (horizon)

max. time step = 1.19 µs
percentage of broken bonds = 99.1 %
max. kinetic energy = unstable
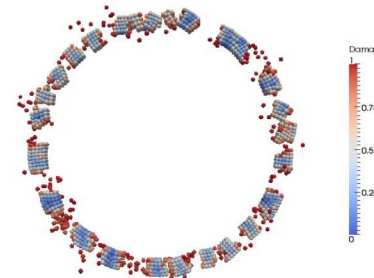
Time step = 5.0 µs
46.7% of bonds broken

Time step = 7.5 µs
62.7 % of bonds broken

Short Course
Peridynamic Theory of Solid Mechanics

Computational Peridynamics

Outline

- Ingredients of a peridynamics simulation
  - Governing equations
  - Constitutive model, bond failure law
  - Contact model
  - Discretization
  - Time integrator
- Surface effect in peridynamic simulations
- Estimation of the maximum stable time step for dynamic simulations
- **Convergence of peridynamic models**
- Demonstration of meshfree peridynamics for model analysis
- Modeling damage and failure

Convergence of meshfree peridynamics

- Two forms of convergence: horizon and mesh spacing
  - Convergence to a local solution as horizon approaches zero
  - Convergence to a nonlocal solution under mesh refinement with horizon held constant
- Current practice introduces errors and spoils convergence
  - Quadrature, poor treatment of neighbor-horizon intersections

Approaches for improving convergence behavior

- Improved treatment of neighbor-horizon intersections
  - Variety of correction techniques (scalar multiplier):
    - PD-LAMMPS, Hu-Ha-Bobaru, analytic partial area (2D)
  - Application of smoothly-decaying influence functions
  - Approximate calculation of partial volumes (3D)
  - Geometry, quadrature
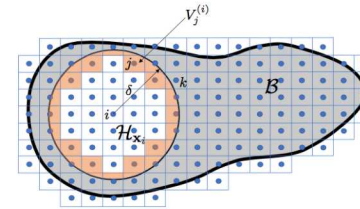
Neighbor-horizon intersection in 2D
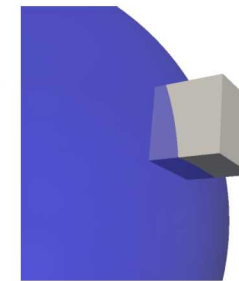
Neighbor-horizon intersection in 3D

Seleson, P. Improved one-point quadrature algorithms for two-dimensional peridynamic models based on analytical calculations, *CMAME*, 282, pp. 184-217, 2014.

Seleson, P., and Littlewood, D.J. Convergence studies in meshfree peridynamic simulations. *Computers and Mathematics with Applications* 71:2432-2448, 2016.

Seleson, P., and David J. Littlewood, D.J. Numerical tools for effective meshfree discretizations of peridynamic models. In George Z. Voyiadjis, editor, *Handbook of Nonlocal Continuum Mechanics for Materials and Structures. Springer. Accepted.*

Numerical experiments: Solution of statics problem with known solution

- Linearized LPS material model equates to classical local model under assumption of a quadratic displacement field

Peridynamic equation of static elasticity, linearized LPS model

$$-\int_{\mathcal{H}_\mathbf{x}} \frac{\omega(|\boldsymbol{\xi}|)}{m} \Big\{ (3K - 5G) \left(\vartheta^{\mathrm{lin}}[\mathbf{x}] + \vartheta^{\mathrm{lin}}[\mathbf{x} + \boldsymbol{\xi}] \right) \boldsymbol{\xi}$$

$$+ 30G \frac{\boldsymbol{\xi} \otimes \boldsymbol{\xi}}{|\boldsymbol{\xi}|^2} (\mathbf{u}(\mathbf{x} + \boldsymbol{\xi}) - \mathbf{u}(\mathbf{x})) \Big\} \mathrm{d}V_{\boldsymbol{\xi}} = \mathbf{b}(\mathbf{x}) \qquad \mathbf{x} \in \Omega,$$

$$\mathbf{u}(\mathbf{x}) = \mathbf{g}(\mathbf{x}) \qquad \mathbf{x} \in \mathcal{B} \setminus \Omega.$$

Classical Navier-Cauchy equation of static elasticity

$$-\left[G \nabla^2 \mathbf{u}(\mathbf{x}) + \left(K + \frac{1}{3}G \right) \nabla (\nabla \cdot \mathbf{u})(\mathbf{x}) \right] = \mathbf{b}(\mathbf{x}).$$

- Permits verification via method of manufactured solutions

Quadratic displacement field

$$u(\mathbf{x}) = U_{11}x^2 + U_{22}y^2 + U_{33}z^2 + U_{12}xy + U_{13}xz + U_{23}yz,$$

$$v(\mathbf{x}) = V_{11}x^2 + V_{22}y^2 + V_{33}z^2 + V_{12}xy + V_{13}xz + V_{23}yz,$$

$$w(\mathbf{x}) = W_{11}x^2 + W_{22}y^2 + W_{33}z^2 + W_{12}xy + W_{13}xz + W_{23}yz,$$

Body force density for static equilibrium

$$b_1 = -\left[2G\left(U_{11} + U_{22} + U_{33} \right) + \left(K + \frac{1}{3}G \right) \left(2U_{11} + V_{12} + W_{13} \right) \right],$$

$$b_2 = -\left[2G\left(V_{11} + V_{22} + V_{33} \right) + \left(K + \frac{1}{3}G \right) \left(U_{12} + 2V_{22} + W_{23} \right) \right],$$

$$b_3 = -\left[2G\left(W_{11} + W_{22} + W_{33} \right) + \left(K + \frac{1}{3}G \right) \left(U_{13} + V_{23} + 2W_{33} \right) \right].$$

Convergence results for different partial-volume schemes and different influence functions
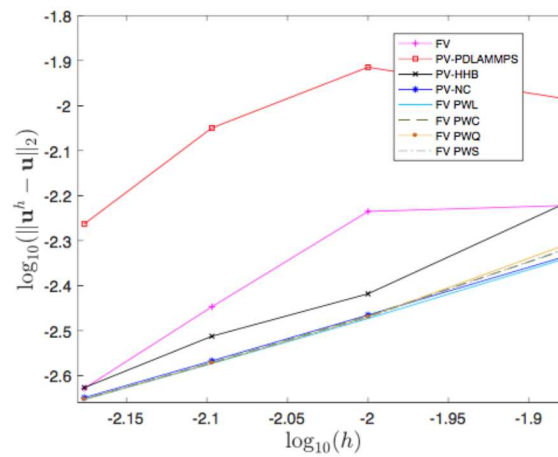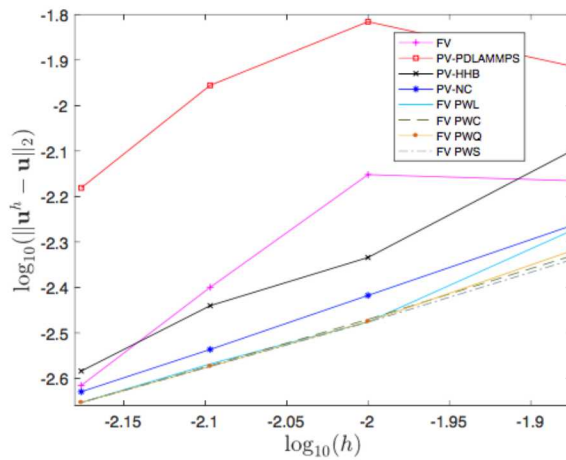
Algorithm	$\alpha = 0$		$\alpha = 1$	
	$\bar{r}$	R	$\bar{r}$	R
FV	1.53	0.165	1.38	0.128
PV-PDLAMMPS	0.86	0.186	0.89	0.167
PV-HHB	1.56	0.035	1.34	0.030
PV-NC	1.22	0.003	1.05	0.001
FV PWL	1.24	0.036	1.05	0.004
FV PWC	1.07	0.005	1.11	0.009
FV PWQ	1.10	0.014	1.15	0.016
FV PWS	1.04	0.006	1.12	0.012

Short Course
Peridynamic Theory of Solid Mechanics

Numerical experiments: Solution of dynamics problem

- Cubic computational domain

- Initial displacement applied to shell of internal nodes

- Wave allowed to propagate freely through domain

- Solutions compared against highly-refined benchmark solution

Initial displacement

Final displacement
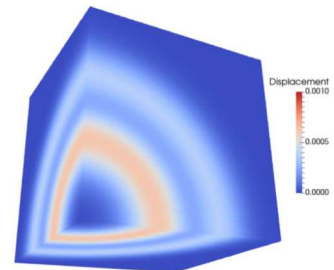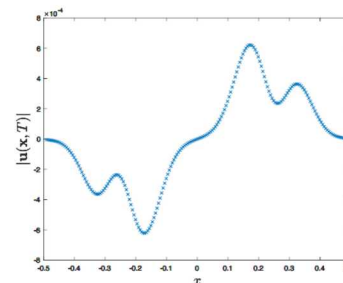
Initial conditions

$$\mathbf{u}_0(\mathbf{x}) = \begin{cases} ae^{-\frac{(|\mathbf{x}|-r_0)^2}{\ell^2}} \dfrac{\mathbf{x}}{|\mathbf{x}|} & \text{if} \quad (r_0 - 3\ell) \leqslant |\mathbf{x}| \leqslant (r_0 + 3\ell) \\ 0 & \text{otherwise,} \end{cases},$$

$$\mathbf{v}_0(\mathbf{x}) = \mathbf{0},$$

Convergence results for different partial-volume schemes and different influence functions
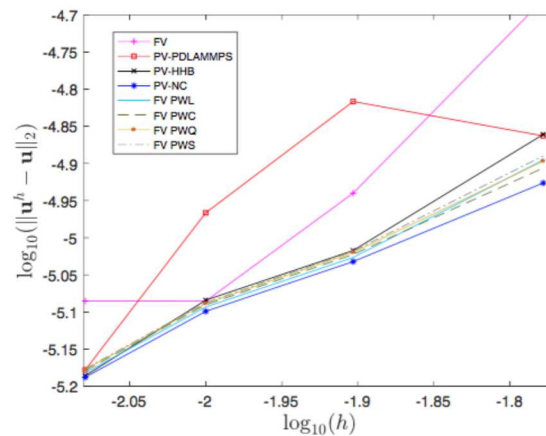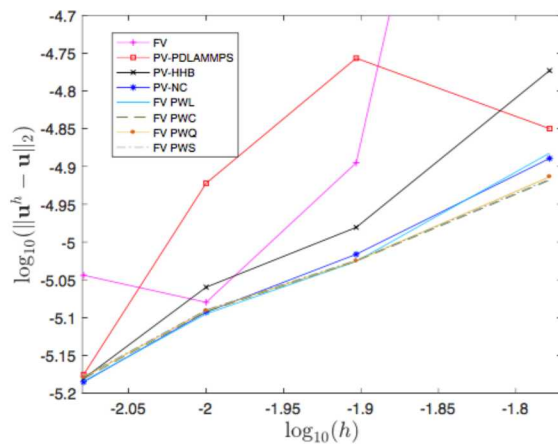
Algorithm	$\alpha = 0$		$\alpha = 1$	
	$\bar{r}$	R	$\bar{r}$	R
FV	4.27	0.514	1.41	0.099
PV-PDLAMMPS	1.05	0.202	1.02	0.157
PV-HHB	1.31	0.038	1.04	0.026
PV-NC	0.96	0.013	0.85	0.016
FV PWL	0.98	0.019	0.93	0.017
FV PWC	0.85	0.016	0.88	0.015
FV PWQ	0.86	0.015	0.91	0.015
FV PWS	0.85	0.016	0.93	0.015

Changing the influence function changes the underlying model (physics)
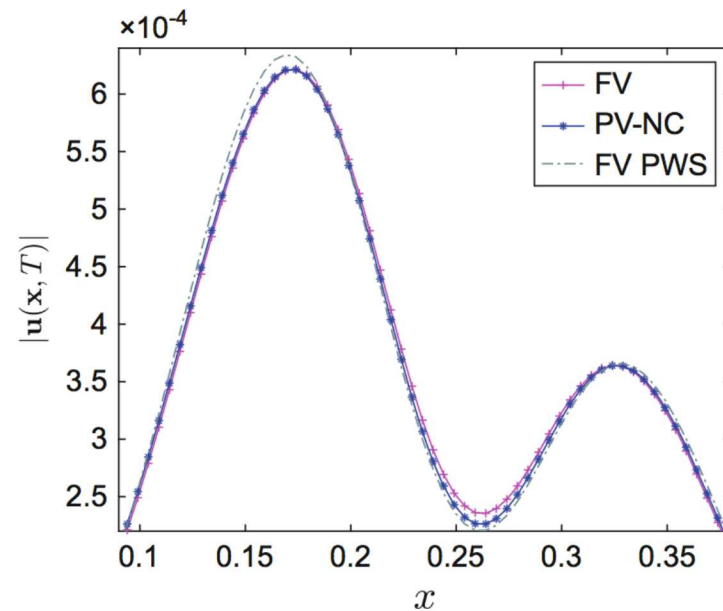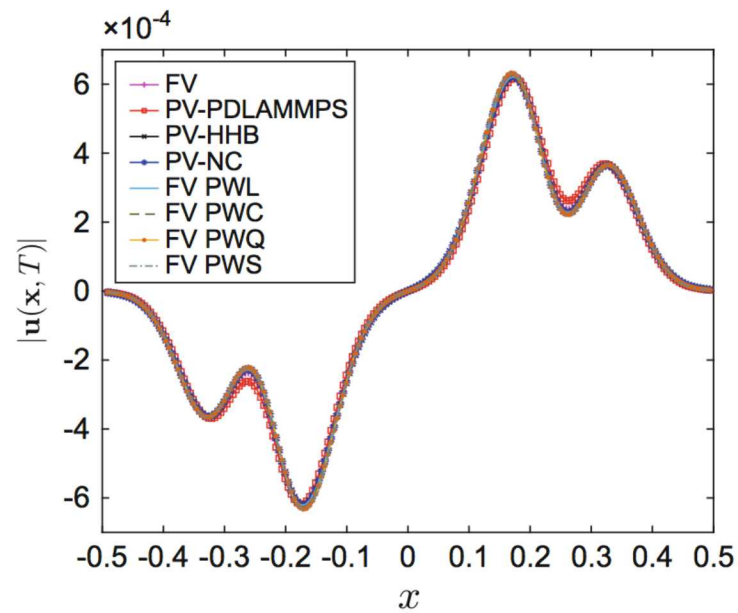
Computational Peridynamics

Outline

- Ingredients of a peridynamics simulation
    - Governing equations
    - Constitutive model, bond failure law
    - Contact model
    - Discretization
    - Time integrator
- Surface effect in peridynamic simulations
- Estimation of the maximum stable time step for dynamic simulations
- Convergence of peridynamic models
- **Demonstration of meshfree peridynamics for model analysis**
- Modeling damage and failure

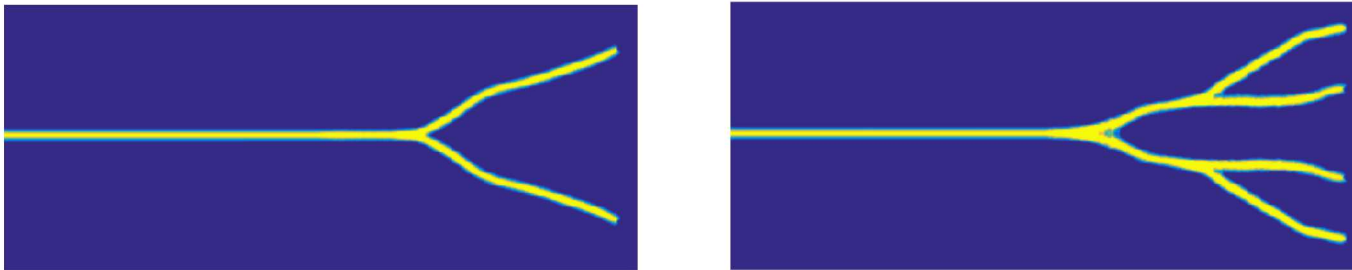Sandia National Laboratories

OAK RIDGE National Laboratory

Why modal analysis?

- Modal analysis is used to determine the dominant structural modes and natural frequencies of a given system

- Peridynamic models containing material damage can be used in the analysis of experimentally-measured frequency responses (nondestructive testing of bridges, etc.)

How does it work?

- Modal analysis is achieved by solving for the dominant eigenvalues and eigenvectors of the tangent stiffness matrix

Test case

One-dimensional analysis of simply-supported beam with square cross section

Classical (local) analytic solution

E	Elastic modulus
h	Height and depth of beam
m	Mass of beam
l	Length of beam
n	Positive integer
f_n	Characteristic linear frequency (mode n)

$$f_n = \frac{n^2 \pi}{2} \sqrt{\frac{E \, h^4}{12 \, m \, l^4}}$$

Results from peridynamic simulation

- Beam dimensions: 1m x 0.01m x 0.01m

- Material: steel (E = 206.8 GPa)

- Peridynamic horizon: 0.000713m

- Correspondence elastic material model

- Beam discretized with 840K elements

Mode	Classical Theory	Peridynamic Simulation	Percent Difference
1	23.30 Hz	23.26 Hz	0.17 %
2	93.22 Hz	93.02 Hz	0.21 %
3	209.73 Hz	209.06 Hz	0.32 %
4	372.86 Hz	371.29 Hz	0.43 %
5	582.59 Hz	579.39 Hz	0.55 %

Visualization of first five mode shapes

(a) Mode 1.
(b) Mode 2.
(c) Mode 3.
(d) Mode 4.
(e) Mode 5.
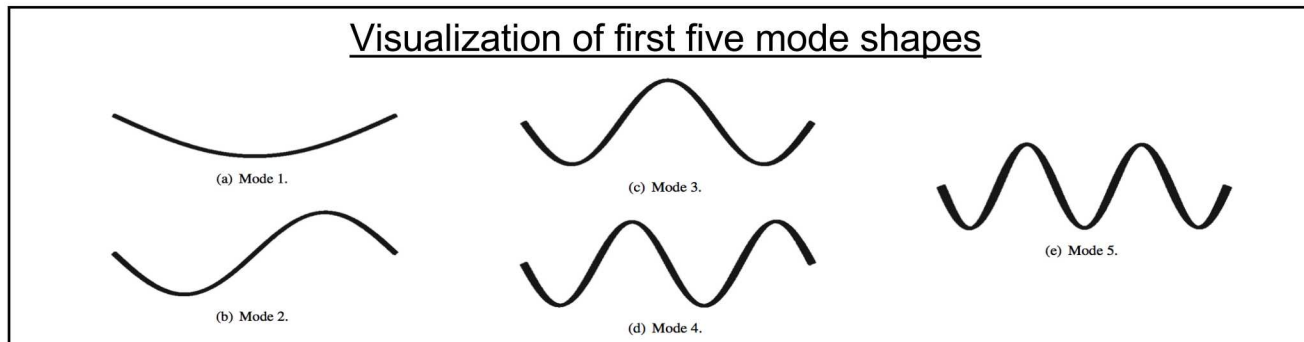
David J. Littlewood, Kyran Mish, and Kendall Pierson. 2012. Peridynamic simulation of damage evolution for structural health monitoring.
Proceedings of the ASME 2012 International Mechanical Engineering Congress and Exposition (IMECE2012), Houston, TX.

Sandia National Laboratories

OAK RIDGE National Laboratory

**Short Course
Peridynamic Theory of Solid Mechanics**

Computational Peridynamics

Outline

- Ingredients of a peridynamics simulation
  - Governing equations
  - Constitutive model, bond failure law
  - Contact model
  - Discretization
  - Time integrator
- Surface effect in peridynamic simulations
- Estimation of the maximum stable time step for dynamic simulations
- Convergence of peridynamic models
- Demonstration of meshfree peridynamics for model analysis
- **Modeling damage and failure**

Modeling failure and damage with peridynamics

- Modeling pervasive damage is a primary advantage of peridynamics

- Nonlocality separates the length scale (horizon) from the mesh, which **relieves mesh dependence**

- **Convergent solutions** to material failure problems (localizing phenomenon) are possible with peridynamics, impossible with a local model

- Cracks develop / grow / branch in peridynamic simulations based primarily on energetics

[Images courtesy Seleson]

Experimental setup

- Tube expansion via collision of Lexan projectile and plug within AerMet tube
- Accurate recording of velocity and displacement on tube surface

Modeling approach

- AerMet tube modeled with peridynamics, elastic-plastic material model with linear hardening
- Lexan plugs modeled with traditional FEM, EOS-enabled Johnson-Cook material model
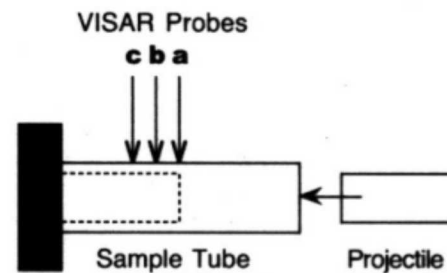
Experimental setup
[Vogler, et al.]

Computational model

Vogler, T.J., Thornhill, T.F., Reinhart, W.D., Chhabidas, L.C., Grady, D.E., Wilson, L.T., Hurricane, O.A., and Sunwoo, A. Fragmentation of materials in expanding tube experiments. *International Journal of Impact Engineering*, 29:735-746, 2003.

D. J. Littlewood. Simulation of dynamic fracture using peridynamics, finite element modeling, and contact. In *Proceedings of the ASME 2010 International Mechanical Engineering Congress and Exposition (IMECE)*, Vancouver, British Columbia, Canada, 2010.
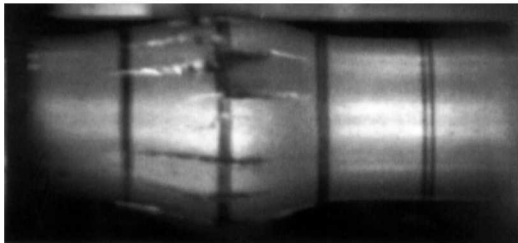
Experimental image at 15.4 microseconds [Vogler et. al]
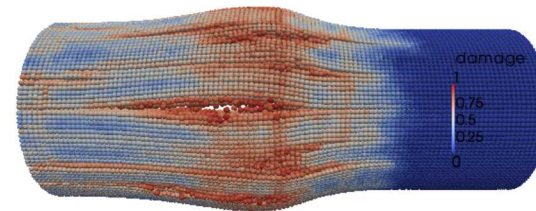
Simulation at 15.4 microseconds
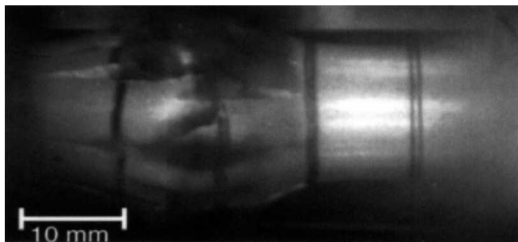
Experimental image at 23.4 microseconds [Vogler et. al]
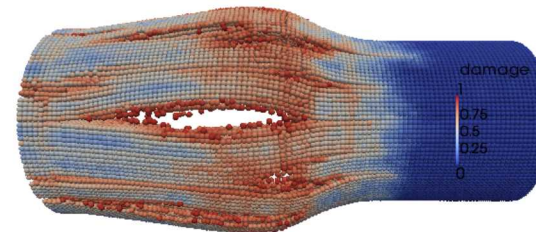
Simulation at 23.4 microseconds

Displacement and velocity
on tube surface
at probe position A
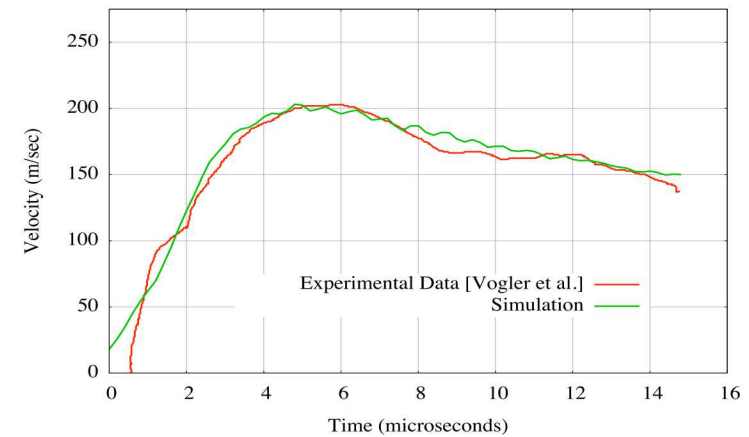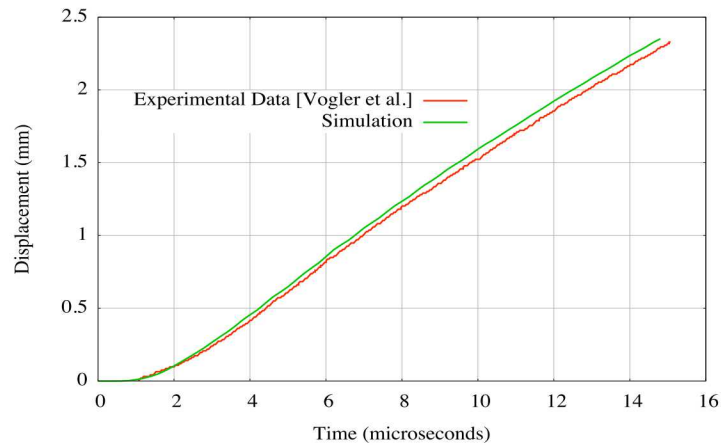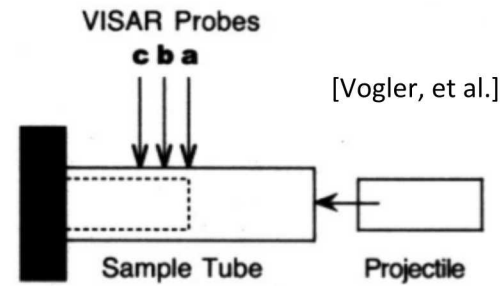
[Vogler, et al.]

Qualitative Comparison of Fragmentation Results

- Vogler et. al reported significant uncertainty in results at late time

- Approximately half the tube remained intact

- Vogler et al. recovered 14 fragments with mass greater than one gram
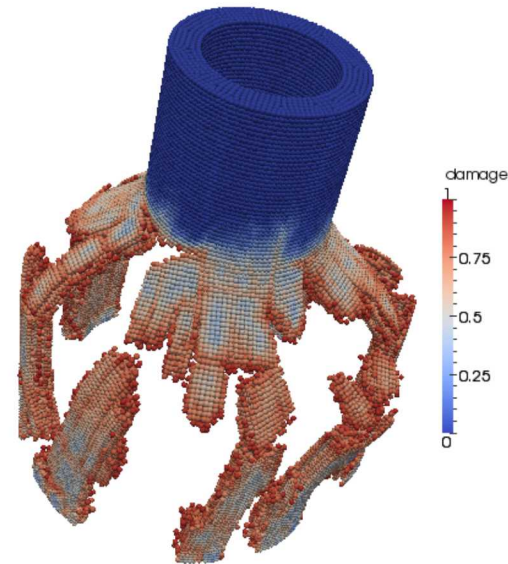
Simulation at 84.8 microseconds

Characterizing fragment data with a Cumulative Distribution Function

- A CDF can be created for any quantity of interest
- Provides insight into the fragmentation process
- Allows for comparison with experimental data

$$P(X) = \frac{1}{M} \sum_{\substack{i=1 \\ X_i \leq X}}^{N_{\mathrm{frag}}} m_i \qquad M = \sum_{i=1}^{N_{\mathrm{frag}}} m_i$$

P(X) is the probability that a given material point belongs to a fragment whose property value X_i is less than X

Example: CDF for fragment mass

Fragments identification in a meshfree peridynamic simulation

- Provide post-processing capability for characterizing fragmentation process

Approach

- Computational domain is traversed to identify networks of unbroken bonds
- Process is iterative, converges when fragment numbers are no longer changing
- A fragment number is assigned to every node in the model
- Tiny fragments are (optionally) combined and assigned a common fragment number
- Related quantities of interest are computed for each fragment
  - Mass, center of mass, linear and angular momentum, moments of inertia, block names
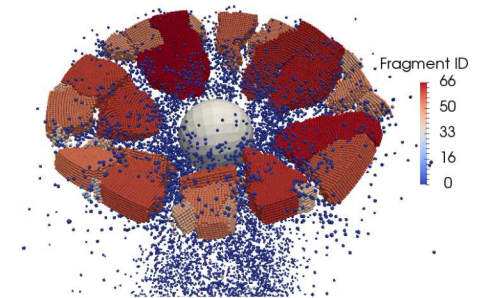
Identification of
disk fragments

DO initialize fragment numbers to node ids
REPEAT until fragment numbers stop changing
  FOR every node i
    FOR all neighbors j of node i
      IF the bond between nodes i and j is unbroken
        DO assign max(F_i , F_j) to nodes i and j

David Littlewood, Stewart Silling, Paul Demmie. 2016. Identification of Fragments in a Meshfree Peridynamic Simulation. Proceedings of the ASME 2016 International Mechanical Engineering Congress and Exposition, Phoenix, Arizona.

Computational Peridynamics
7. Modeling failure and damage

- Elastic sphere impacting a brittle elastic disk
- Projectile modeled with classical FEM
  - Elastic material model
  - Radius 5.0 mm,
  - Initial velocity 35.0 m/s
- Target modeled with peridynamics
  - Bond-based microelastic material model
  - Critical stretch bond failure rule
  - Radius 17.0 mm, height 2.5 mm

Damage
- 1.00
- 0.75
- 0.50
- 0.25
- 0.00
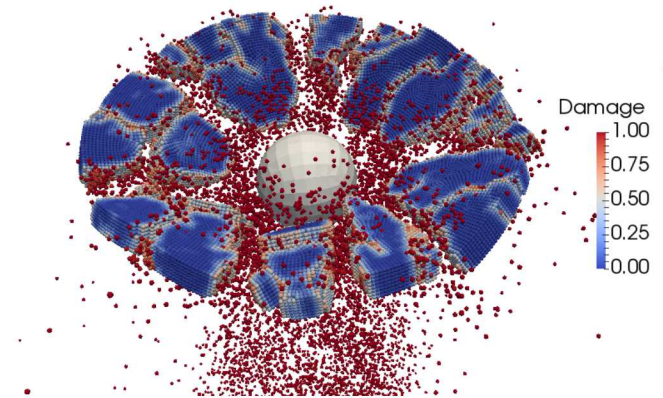
Material parameters
for projectile

Parameter	Value
Density ρ	993.1 kg/m^3
Bulk modulus k	1.0 GPa
Poisson's ratio ν	0.3

Material parameters
for target

Parameter	Value
Density ρ	2200.0 kg/m^3
Bulk modulus k	14.9 GPa
Horizon δ	1.0 mm
Critical stretch s_{crit}	0.0005

Parameters for
fragment identification

output file = frag_data.csv

increment = 4.0e-5

minimum fragment size = 5

Sandia National Laboratories

OAK RIDGE National Laboratory

Short Course
Peridynamic Theory of Solid Mechanics

Algorithm captures evolution of fragmentation process

Exclusion of tiny fragments has a significant effect
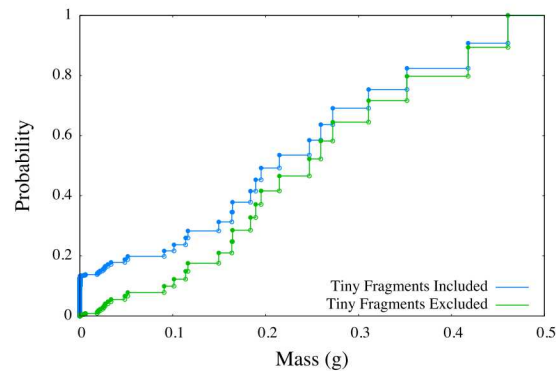
Threshold Fragment Size	Total Mass of Tiny Fragments
1	0.000 g
2	0.531 g
3	0.613 g
4	0.641 g
5	0.651 g

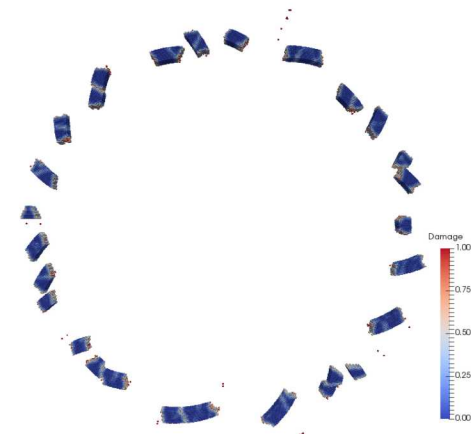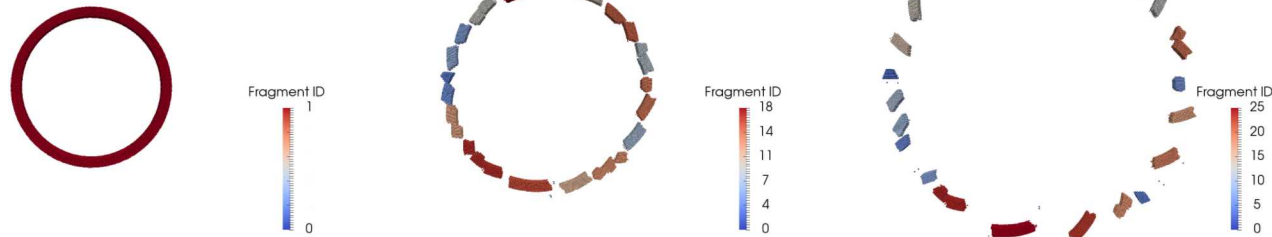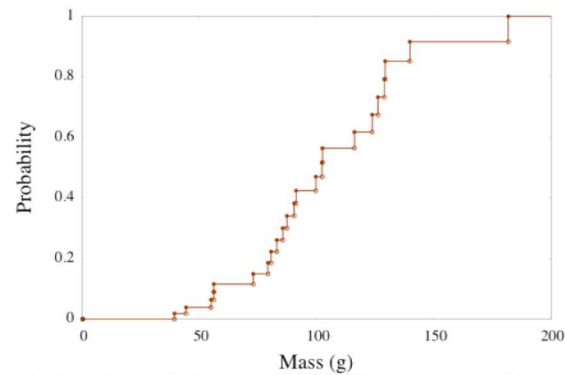**Short Course**
Peridynamic Theory of Solid Mechanics

- Fragmentation of an expanding ductile ring

- Bond-based microplastic material model

- Critical stretch bond failure rule

- Inner radius 110.0 mm, outer radius 125.0 mm, height 25.0 mm

- Initial outward radial velocity 100.0 m/s

- ~60,000 nodal volumes

Discretization of ring

Material parameters

Parameter	Value
Density ρ	$7850.0\,\mathrm{kg/m^3}$
Bulk modulus k	$140.0\,\mathrm{GPa}$
Horizon δ	$5.025\,\mathrm{mm}$
Yield stretch s_Y	0.000988
Critical stretch s_{crit}	0.02

Parameters for
fragment identification

output file = frag_data.csv

increment = 2.4e-5

minimum fragment size = 0

Algorithm captures evolution of fragmentation process

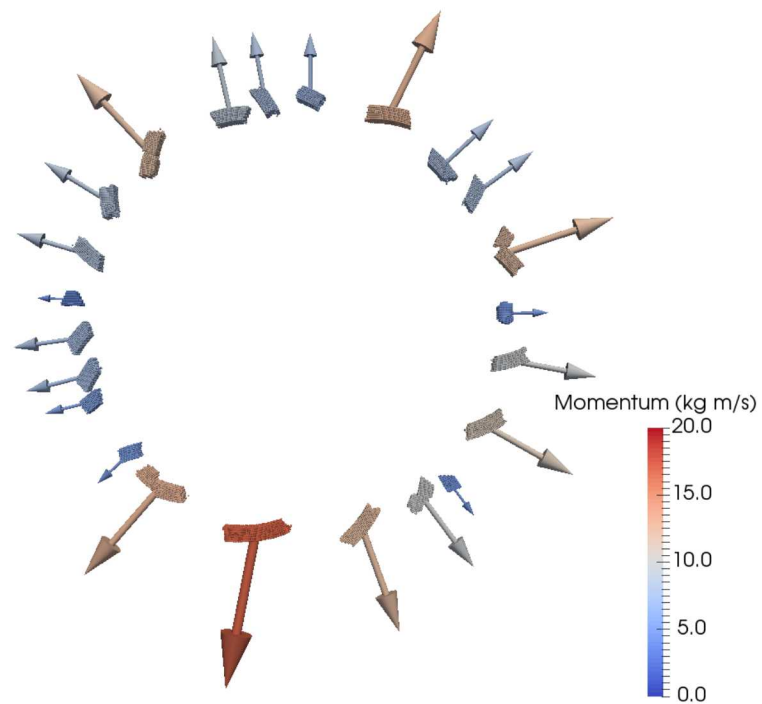*Exclusion of tiny fragments does not affect results*

Visualization of
fragment momentum

The Peridigm peridynamics code

http://peridigm.sandia.gov

https://github.com/peridigm/peridigm
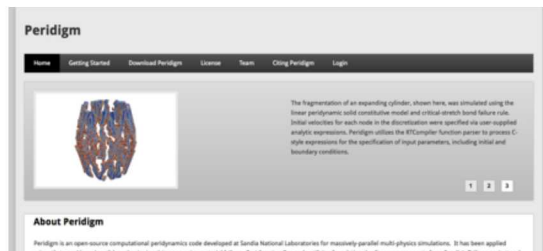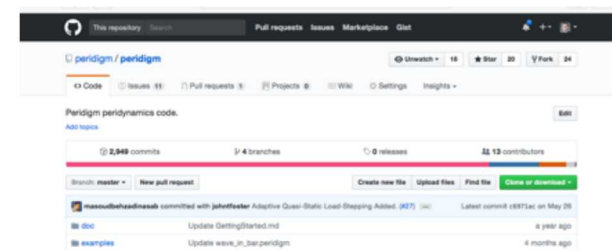
Map of downloads from
peridigm.sandia.gov